



Finger vein recognition using weighted local binary pattern code based on a support vector machine^{*}

Hyeon Chang LEE¹, Byung Jun KANG², Eui Chul LEE³, Kang Ryoung PARK^{†‡1}

⁽¹⁾Division of Electronics and Electrical Engineering, Dongguk University, Seoul 100-715, Korea)

⁽²⁾Electronics and Telecommunications Research Institute, Daejeon 305-700, Korea)

⁽³⁾Division of Fusion and Convergence of Mathematical Sciences, the National Institute for Mathematical Sciences, Daejeon 305-340, Korea)

[†]E-mail: parkgr@dongguk.edu

Received Sept. 5, 2009; Revision accepted Feb. 1, 2010; Crosschecked June 9, 2010

Abstract: Finger vein recognition is a biometric technique which identifies individuals using their unique finger vein patterns. It is reported to have a high accuracy and rapid processing speed. In addition, it is impossible to steal a vein pattern located inside the finger. We propose a new identification method of finger vascular patterns using a weighted local binary pattern (LBP) and support vector machine (SVM). This research is novel in the following three ways. First, holistic codes are extracted through the LBP method without using a vein detection procedure. This reduces the processing time and the complexities in detecting finger vein patterns. Second, we classify the local areas from which the LBP codes are extracted into three categories based on the SVM classifier: local areas that include a large amount (LA), a medium amount (MA), and a small amount (SA) of vein patterns. Third, different weights are assigned to the extracted LBP code according to the local area type (LA, MA, and SA) from which the LBP codes were extracted. The optimal weights are determined empirically in terms of the accuracy of the finger vein recognition. Experimental results show that our equal error rate (EER) is significantly lower compared to that without the proposed method or using a conventional method.

Key words: Finger vein recognition, Support vector machine (SVM), Weight, Local binary pattern (LBP)

doi: 10.1631/jzus.C0910550

Document code: A

CLC number: TP391

1 Introduction

As security requirements increase, biometric techniques, including face, fingerprint, iris, voice, and vein recognitions, have been widely used for personal identification (Jain *et al.*, 2004). Biometrics has been applied to building access control, immigration control, and user authentication for financial transactions. Although vein recognition has not been as widely adopted as fingerprint, face, and iris recognition, it has some advantages. Since vein patterns exist inside

the skin, it is very difficult to steal them. In addition, the vein patterns are not easily altered by other factors such as dry or wet skin (Wang and Leedham, 2006; Watanabe, 2008). Retina vein recognition is one form of vein pattern recognition, which identifies a user based on retinal vascular patterns. Since a view of the retinal veins is contained within the pupil, a special camera device is required to obtain the vein patterns and the user must place his/her eye close to the camera (Usher *et al.*, 2008; Sukumaran and Punithavalli, 2009). Vein patterns on the back of the hand have been adopted for matching in hand vascular identification (Ding *et al.*, 2005; Ferrer *et al.*, 2009). Palm vein recognition, investigated in previous studies, uses vein patterns in the palm for personal identification (Lin and Fan, 2004; Watanabe, 2008). Hand and palm vein recognitions, however, have a disadvantage

[‡] Corresponding author

^{*} Project (No. R112002105070020(2010)) supported by the National Research Foundation of Korea (NRF) through the Biometrics Engineering Research Center (BERC) at Yonsei University

© Zhejiang University and Springer-Verlag Berlin Heidelberg 2010

in that the dimensions of the device are inevitably large because the vascular features from the whole hand are extracted while capturing a vein image. To overcome this problem, many researchers have investigated the biometrics of finger veins (Miura *et al.*, 2004; 2007; Zhang *et al.*, 2006; Choi *et al.*, 2009). In Yanagawa *et al.* (2007), for example, the finger vasculature was known to be a high security level biometric due to the pattern richness. The vein patterns of each finger from a given person are known to differ from each other. There are two categories of previous finger vein recognition algorithms: one that adopts the local vein shape and one that uses the holistic vein texture. The finger vein recognition algorithms based on the local vein shape have included the finger vein extraction process. Miura *et al.* (2004) introduced the method to locate finger vein patterns. It uses the iterative procedure for tracing vein lines. They took advantage of the characteristic that a finger vein is continuously connected. In their experiments with 678 images, the error of vein recognition (the equal error rate, EER) was 0.145% (Miura *et al.*, 2004). In later research by Miura, the vein was located with information from a cross-sectional contour (Miura *et al.*, 2007). In general, the finger vascular region is darker than the skin area, and the cross-sectional contour of the finger vein is represented as a valley. Based on this property, Miura *et al.* (2007) detected the vein position at which the calculated curvature value reached a maximum based on the cross-sectional profiles in four directions. They obtained an EER of 0.0009% in experiments with 678 finger vein images. Also, Choi *et al.* (2009) introduced a new method for finger vascular extraction. In their research, the vein image from the same finger was known to be altered by uneven illumination and changes in physical condition. To overcome these problems, they used gradient normalization, curvature calculation, and binarization. Gradient normalization makes the curvature of a vein pattern fairly uniform. This method requires, however, considerable processing time for finger vein extraction. The accuracy of finger vein extraction is reduced when the finger vein image captured is of low quality; thus, recognition accuracy can be also reduced. Finger vein recognition algorithms based on the holistic vein texture do not perform finger vein extraction (Jang YK *et al.*, 2008; Lee *et al.*, 2009), so they need less processing time.

Jang YK *et al.* (2008) proposed a local binary pattern (LBP) based identification method of finger vascular patterns. They segmented the foreground area of the finger and normalized it into 50×20 pixels. Without extracting a finger vein, they performed finger vein recognition by extracting LBP codes from the normalized image. They found, however, that LBP-based finger vein recognition had a lower accuracy than finger vein recognition based on the local vein shape because the LBP codes were taken from both the finger skin and the finger vein regions. Therefore, they discriminated between the finger vein region and the skin region based on the standard deviation in a local area of 3×3 pixels. They did not use the LBP codes extracted from the finger skin region for both enrollment and recognition. The finger vein region and skin region, however, were not completely discriminated by using the standard deviation, because the boundary between the finger vein region and the skin region was indistinct in the captured image. This caused incorrect classification between the finger vein and skin regions, which decreased the recognition accuracy. Lee *et al.* (2009) proposed a method of reducing the positional disparities of the vein images with the minutiae of vein, matching based on LBP. They also adopted a simple method of discriminating vein and skin regions based on the standard deviation obtained in a similar fashion.

To solve the above-noted problems, a new identification method of finger vascular patterns is proposed using weighted LBP codes based on a support vector machine (SVM). This research is novel in the following three ways. First, the holistic texture codes are extracted from the finger vein region using the LBP method without the vein detection procedure. This can reduce the processing time and the complexities of detecting the finger vein patterns. Second, we classify the local areas from which the LBP codes are extracted into three categories based on an SVM classifier: local areas including a large amount (LA), a medium amount (MA), and a small amount (SA) of vein patterns. Third, different weights are assigned to the extracted LBP code according to the types of local areas (LA, MA, and SA) in which the LBP codes are extracted. The optimal weights are determined empirically in terms of the finger vein recognition accuracy.

2 The proposed method

2.1 Introduction of the proposed method

Our method is depicted in Fig. 1. First, the finger vein image is acquired, as shown in Fig. 2 (Jang YK *et al.*, 2008; Lee *et al.*, 2009). The foreground area of the finger is segmented using masks (Fig. 3). The segmented finger region is then normalized into 150×60 pixels, and then sub-sampled to 50×20 through average filtering with 3×3 mask considering real-time processing. For brightness normalization of the sub-sampled image, histogram stretching and the shifting of the mean gray value are performed. Then, the LBP codes are extracted from the 3×3 local area, and then we give different weights to the LBP codes according to the LA, MA, and SA. For classifying the local areas into LA, MA, and SA, we use the SVM based on the mean and standard deviations of the gray values in the local area. Finally, authentication is performed by calculating the hamming distance (HD) between the weighted LBP codes of registered and currently captured finger vein images.

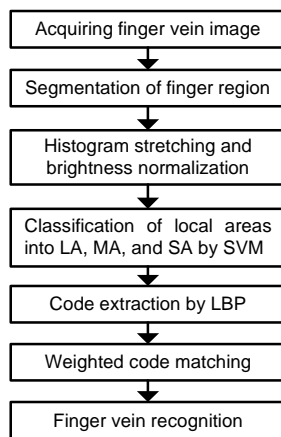


Fig. 1 The overall procedure of the proposed method

2.2 Acquiring the finger vein image

As shown in Fig. 2, the device is designed to minimize the contact area of the finger. Thus, our device has two advantages over conventional finger vein capturing devices. First, it does not maintain a latent fingerprint on the sensor surface. Second, it can reduce user's discomfort by reducing sensor contact.

The proposed device uses a charge-coupled device (CCD) Web camera (Fig. 2a) that has a universal serial bus (USB) interface (Quickcam Pro 4000,

<http://www.logitech.com/index.cfm/432/269>). Since the finger vein pattern is visible using near-infrared (NIR) light, the visible light passing filter of the Web camera was removed. An NIR passing filter is included inside the camera. In this case, the NIR filter passes NIR light with wavelengths greater than 750 nm.

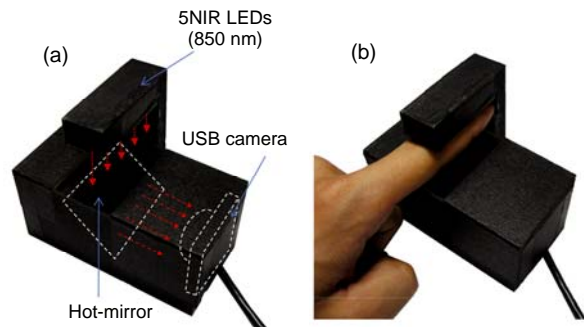


Fig. 2 The proposed device for acquiring the finger vein image (Lee *et al.*, 2009)

(a) Device structure; (b) Using the device

To make the finger vein pattern distinctive, an additional 5 NIR light emitting diodes (LEDs) are attached to the upper part of the device, as shown in Fig. 2a (Lee *et al.*, 2009). The gray level of finger vein is lower compared to the skin area because the hemoglobin in the vein accepts more NIR light than the other tissues (Wang and Leedham, 2006). In general, arteries have oxygenated hemoglobin and veins have deoxygenated hemoglobin. NIR light with a wavelength greater than 760 nm is absorbed in deoxygenated hemoglobin. The NIR light with a wavelength around 930 nm is absorbed best (Watanabe, 2008). The sensing ability of a conventional charge-coupled device (CCD) sensor, however, is degraded according to the increase in the wavelength of the NIR light. In more detail, the image brightness recorded by the CCD camera with a 930 nm wavelength is darker than that recorded with the wavelength of 760 nm. Thus, considering the trade-off between the image brightness caused by the sensing ability of the CCD sensor and the absorption amount of deoxygenated hemoglobin, we chose the 850 nm wavelength NIR illuminators by experimentation.

A hot-mirror was used in the proposed device. The hot-mirror has the characteristics of reflecting the NIR light and transmitting the visible light. Based on that, the hot mirror, which is slanted at 45° , was positioned in front of the USB camera (Fig. 2a). As a

result, the height of the device was reduced. Consequently, the size and cost of the proposed device were much reduced.

2.3 Segmentation of the finger region

After capturing a finger vein image, we segmented the finger region by using masks in Fig. 3 and the upper and lower boundaries of the finger region were easily detected. Based on the convolution value of the mask in Fig. 3, the boundary position of the finger was segmented. This procedure was iterated at each X position and thus the consequent boundary lines were obtained (Jang YK *et al.*, 2008; Lee *et al.*, 2009).

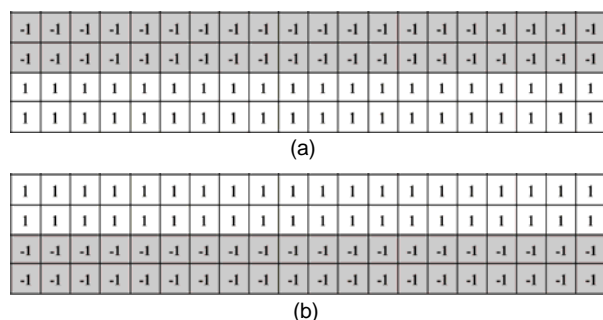


Fig. 3 The finger detection masks for (a) the uppermost and (b) the lowermost boundary of the finger (Jang YK *et al.*, 2008; Lee *et al.*, 2009)

Fig. 4 shows some examples of the finger regions that are segmented using masks. We normalized the segmented finger region into 150×60 pixels to reduce the variations of the magnification factor of the finger in the image. This size normalization was achieved by linear stretching of the foreground area of the finger. Fig. 5 shows the stretched images. Finally, it is sub-sampled to the image whose size is one third of the stretched image in both horizontal and vertical directions, through average filtering with 3×3 mask, to reduce computation time and noise components (Jang YK *et al.*, 2008; Lee *et al.*, 2009).

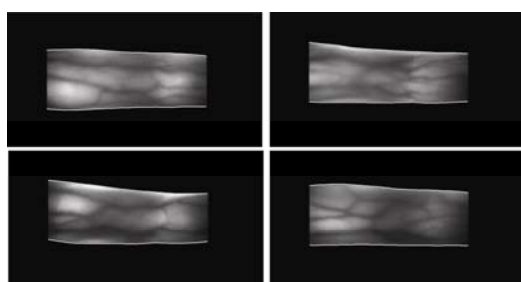


Fig. 4 The image results of the segmented finger region

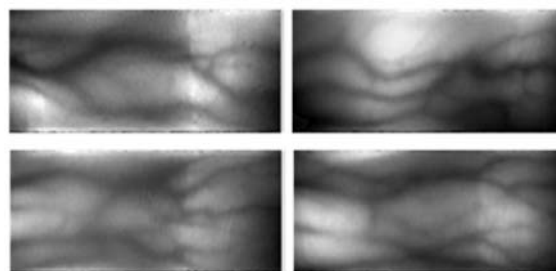


Fig. 5 Examples of the stretched image

2.4 Histogram stretching and brightness normalization

In general, the finger thickness affects the variations of the image brightness. The smaller the finger thickness, the higher the brightness of the finger vein image. An SVM was used to classify the local area of 3×3 pixels into the LA, MA, and SA. These are the local areas including an LA, an MA, and an SA of vein patterns. Because the SVM is a supervised learning method and the mean gray value of the local area is used as one of the feature values, brightness normalization is a very important procedure for obtaining an optimal classification. Histogram stretching and the shifting of the mean gray values were performed for the brightness normalization. Here, the shifting of the mean gray values corresponds to the adjustment of the direct current (DC) level of the gray values from the 3×3 local area.

2.5 Classification of the local areas by support vector machine

The conventional SVM is used for two-class separation. Different from the multi-layered perceptron, the optimal classifier of the SVM is defined using the support vectors that exist near the optimal classifier line instead of the whole training data (Vapnik, 1998; Jang J *et al.*, 2008).

The region of the finger vein is difficult to distinguish from that of the finger skin because a diffusion of the infrared light occurs as it passes through the finger. We classified the local area of 3×3 pixels into LA, MA, and SA using the SVM (Fig. 6). Jang YK *et al.* (2008) performed code matching without the classification of finger regions into the three categories. They classified the region into only vein and skin areas based on the standard deviation, which was calculated from the local area of 3×3 pixels where the LBP codes were located. The LBP codes

extracted from the skin area were not used for code matching. Both the vein and skin textures have meaning, however, for the discriminating users. In addition, the capability of the discriminating users for the vein area is changed according to the amount of the included vein pattern. Based on this, we introduced the method of pre-classification of the local area of 3×3 pixels (in which the LBP codes are extracted) into the three categories LA, SA, and MA, based on the SVM classifier.

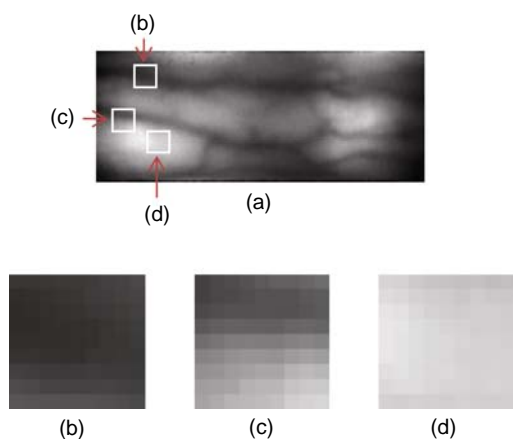


Fig. 6 Three classes of the weighted local binary pattern
(a) Finger region; (b) Large amount (LA) class; (c) Medium amount (MA) class; (d) Small amount (SA) class

The LA category designates that the local area has a large amount of vein (Fig. 6b). The SA category has a small vein pattern in the local area (Fig. 6d). The MA category is used when the number of finger vein pixels is similar to that of the finger skin pixels in the local area (Fig. 6c). If the number of the dark pixels whose gray level is less than the predetermined threshold is greater than 70% of the total pixel number in the local area, the area is determined to be an LA. If the number of the dark pixels whose gray level is less than the predetermined threshold is less than about 30% of the total pixel number in the local area, the area is determined to be an SA. In any other case, the area is determined to be an MA. The predetermined threshold and the 30% and 70% thresholds were determined by experiment. As shown in Fig. 6, the LA class has a low mean gray value and standard deviation, the MA class has a medium mean gray value and high standard deviation, and the SA class has a high gray value and low standard deviation.

To train the SVM, we manually classified the local areas of a finger region into LA, MA, and SA. To better discriminate the local area, we selected a local area in the finger vein image of 150×60 pixels (Fig. 6a) instead of the sub-sampled image of 50×20 pixels. Because the LBP codes are extracted in the sub-sampled image of 50×20 pixels, the mean and standard deviation values for the SVM training were calculated in the local area of the sub-sampled image of 50×20 pixels corresponding to that manually selected in the finger vein image of 150×60 pixels.

Fig. 7 shows the distributions of the LA, MA, and SA classes according to the mean gray values and the standard deviations obtained from 598 local areas of training data. Almost 43% of the whole database was selected for training. The others were used for testing. Based on the distributions in Fig. 7, the optimal classifiers that discriminated classes LA, MA, and SA were obtained by using SVM. A conventional SVM was used for the two-class classification and the MA class was the overlapped area of the LA and SA classes in Fig. 7. Thus, the following hierarchical methods were adopted to obtain the optimal classifiers. At first, the SVM classifier that discriminated class LA and the others including classes MA and SA were trained. Then, a second SVM classifier, which discriminated the SA class, and two others for classes LA and MA, were trained.

The mySVM software was used (Solla *et al.*, 2000; Jang J *et al.*, 2008). Dot, polynomial, radial base, neural, and ANOVA kernels were used as SVM kernels for training. The radial base kernel with a gamma of 5 was selected to be the optimal kernel of two of the SVM classifiers.

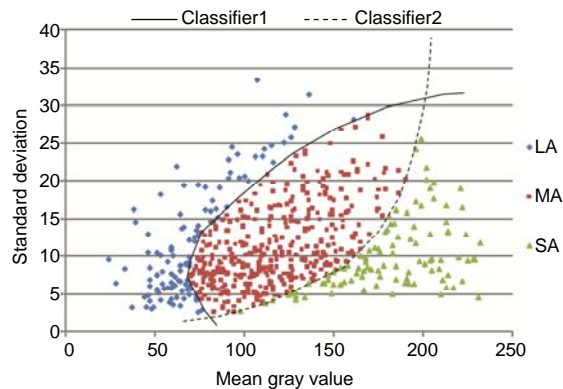


Fig. 7 SVM classifications of data for large amount (LA), medium amount (MA), and small amount (SA) classes

2.6 Code extraction by local binary pattern

The LBP operator was used for feature extraction in face and iris recognition because it is robust to illumination variances (Ahonen *et al.*, 2006; Yang and Wang, 2007; Guo and Jones, 2008). It is expressed as Eqs. (1) and (2) (Ojala *et al.*, 1996; 2002; Jang YK *et al.*, 2008; Lee *et al.*, 2009):

$$\text{LBP}(x_a, y_a) = \sum_{n=0}^7 s(p_n - p_c) \cdot 2^n, \quad (1)$$

$$s(x) = \begin{cases} 1, & x \geq 0, \\ 0, & x < 0, \end{cases} \quad (2)$$

where p_c and p_n denote the gray value of the middle pixel and those of the surrounding ones inside the local area, respectively. For example, in Fig. 8, the p_c is 97. $p_0, p_1, p_2, \dots, p_7$ are 82, 75, 84, 95, 113, \dots , 92, respectively. In the case that $n=0$, $s(p_n - p_c) \cdot 2^n$ is $s(82-97) \cdot 2^0$. Based on Eq. (2), $s(82-97)$ is 0.

Consequently, $s(82-97) \cdot 2^0$ becomes 0. With the same method, in the case that $n=1$, $s(75-97)$ is also 0 and $s(75-97) \cdot 2^1$ is 00 since 2^1 is 10. In the case that $n=2$, $s(84-97)$ is also 0 and $s(84-97) \cdot 2^2$ is 000 since 2^2 is 100. From that, we obtain the binary code of 01110000 (Fig. 8).

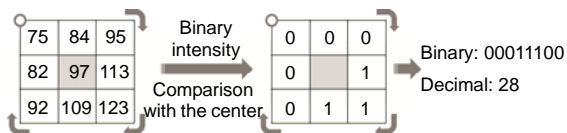


Fig. 8 The local binary pattern (LBP) operator (Jang YK *et al.*, 2008; Lee *et al.*, 2009)

The LBP codes are extracted as 8 bits by the difference between the neighboring pixel and center pixel in the local area. Its size is 3×3 pixels. The local mask for the extraction of the LBP codes is moved in the horizontal and vertical directions with an overlap in the sub-sampled image of 50×20 pixels. Consequently, the total number of bits of the LBP codes extracted from the sub-sampled image of 50×20 pixels equals 6912 (Jang YK *et al.*, 2008; Lee *et al.*, 2009).

The extracted 6912-bit binary codes represent the texture of the finger area including the veins and skin. These codes are matched with the enrolled ones through the operation of hamming distance (HD) (see

Eq. (3) on the next page). Since the HD performs the exclusive-OR operation between the enrolled codes and those from the input image, if they are different (for example, the enrolled code is 0, but the input one is 1, or the registered one is 1, but the input code is 0), the HD increases. Thus, if the enrolled codes and those of the input image come from the same user, the HD is smaller; if the enrolled codes and those of the input image come from a different user, the HD is greater. The bits thus show the similarity of texture between the enrolled image and the input one.

In Jang YK *et al.* (2008), the vascular code bits of vein area were discriminated from those of skin with control codes and LBP. The codes of a 3×3 area are all 1 if they are extracted from vein regions, and the codes are all 0 if they are extracted from skin regions. That is, if the 3×3 area for extracting the LBP codes is determined to be the vein region, the control codes become 11111111. If the 3×3 area for extracting LBP codes is determined to be the skin region, the corresponding control codes become 00000000. The standard deviations of the 3×3 area are used as a criterion of distinguishing vein and skin regions (Jang YK *et al.*, 2008). If the area includes the vein pattern, the standard deviation is greater; if it includes only the skin, the standard deviation is smaller.

Therefore, the previous work of Jang YK *et al.* (2008) needed LBP codes of 6912 bits and control codes of 6912 bits for personal identification. As mentioned previously, because the region of finger vein is difficult to distinguish from that of the finger skin, the local areas are classified into the LA, MA, and SA using the SVM. Thus, the flags of the LA, MA, and SA are defined as 2 (10), 1 (01), and 0 (00), respectively, to distinguish between them. As shown in Fig. 9, the flags are produced as 2 bits per local area of 3×3 pixels; thus, the proposed method needed LBP codes of 6912 bits and control codes of 1728 ($6912/8 \times 2$) bits for personal identification. A total of 8 bits are extracted from each local area of 3×3 pixels in Fig. 8. Thus, the number of bits is $6912/8$. In each of the 8 bits from the local area of 3×3 pixels, the flags of 2 bits are used for discriminating the type of local area as LA, MA, and SA. Thus, the number of control codes is 1728 ($6912/8 \times 2$) bits. Consequently, the total code length is decreased by 37.5% ($[(6912 \times 2) - (6912 + 1728)] \times 100 / (13824) \times 100\%$) in comparison with the previous work.

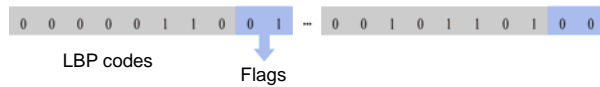


Fig. 9 Extracted local binary pattern (LBP) codes of the 3×3 local area with flags

2.7 Weighted code matching and finger vein recognition

The HD was used as the dissimilarity measure between the enrolled code and the code of an input image. When calculating the HD, we gave a different weight to the LBP codes according to the LA, MA, and SA. The HD is represented as

$$HD = \frac{1}{N} \left\| w_i (\text{codeA} \otimes \text{codeB}) \right\|, \quad (3)$$

where codeA and codeB are the enrolled and the input codes, respectively, and \otimes denotes an exclusive-OR operator.

In addition, the w_i denotes a weight which is determined in Fig. 10. While extracted codes of the input image are matched with the enrolled codes, we multiplied the matching result by the weights determined by the enrolled control codes and those of the input image. These weights w_1 – w_6 were empirically determined in terms of the EER of finger vein recognition.

		Enrolled control codes		
		SA(00)	MA(01)	LA(10)
Control codes of the input image	SA(00)	w_1	w_5	w_4
	MA(01)	w_5	w_2	w_6
	LA(10)	w_4	w_6	w_3

Fig. 10 The weights determined by the enrolled and input control codes

3 Experimental results

We collected finger vein images for experiment. The number of subjects was 120 and finger vein images were obtained from eight fingers of each subject. The two thumbs were excluded because they are too short to capture by the proposed capture device. Previous studies did not use thumbs for the same reason

(Zhang et al., 2006; Miura et al., 2007; Yanagawa et al., 2007; Jang YK et al., 2008; Lee et al., 2009). In addition, 10 finger vein images per finger were captured within a given time interval. Therefore, the database consisted of a total of 9600 finger vein images made up of 640×480 pixels and an 8-bit gray level. Fig. 11 shows some examples of finger vein images.

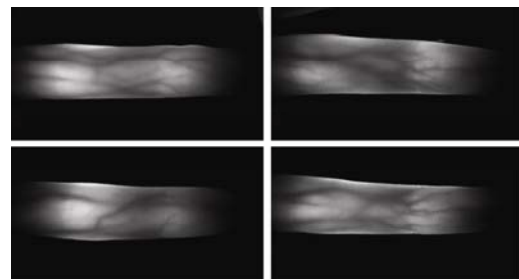


Fig. 11 Examples of the finger vein images of four different users

To enhance the experimental confidence level, we performed cross-validation tests. That is, 43% of the images were randomly selected from the databases for training. The others were used for testing. This procedure was iterated 10 times and the average value of the 10 trials was used to ensure the final accuracy.

We empirically determined the optimal weights w_1 – w_6 of Fig. 10 in terms of the accuracy of verification. The EER was minimized to 0.049% when the w_1 to w_6 were 0.1, 0.6, 0.7, 0.9, 0.5, and 0.6, respectively. The LA class is the most important feature in finger vein recognition because this class determines that the local area includes many finger vein pixels. The SA class is a less important feature because this class represents a local area with few finger vein pixels. So when the HD is calculated between the extracted codes of the input image and the enrolled codes, the weights related to the LA class such as w_3 , w_4 , and w_6 of Fig. 10 become greater than other weights.

The recognition accuracy of the proposed method is compared to previous studies. As mentioned before, previous finger vein recognition algorithms can be divided into two categories: one uses the holistic vein texture and the other uses the local vein shape. The previous method, based on the holistic vein texture, performed personal identification with simple LBP codes after discriminating the finger vein region and skin region by standard deviation in the

local area whose size is 3×3 pixels. If both the enrolled and input vein codes were extracted from the skin region, they were not used for code matching (Jang YK *et al.*, 2008). The previous study, based on local vein shape, performed personal identification using the modified Hausdorff distance after extracting the finger vein features. These are ridges, bifurcation, and endings (Kang and Park, 2009). The distance of two minutia point sets of the finger vein images was calculated by using the modified Hausdorff distance (MHD). Since the Hausdorff distance is sensitive to small perturbations or noise due to the use of summation of maximum distances (Huttenlocher *et al.*, 1993), this approach is not adequate for finger vein features with significant noise levels. To deal with such cases, the MHD was adopted (Dubuisson and Jain, 1994). $P = \{x_1, x_2, \dots, x_m\}$ is extracted from the input image; $Q = \{y_1, y_2, \dots, y_i\}$ is extracted from the enrolled image. Each component of the two sets is a minutia point. The input image is determined as genuine or imposter by comparing the MHD to the threshold (Kang and Park, 2009; Lee and Park, 2009).

$$\text{MHD}(P, Q) = \frac{1}{m} \sum_{x_i \in P} \min_{y_j \in Q} \|x_i - y_j\|. \quad (4)$$

The proposed method does not extract only the vein patterns. Instead, it uses all the information of the texture of the finger from vein and skin. The codes extracted by the LBP are shown from thick vein, thin vein, and skin areas, respectively, in Fig. 12. The HD between the thick vein area (Fig. 12a) and the skin (Fig. 12c) was 0.75. That between the codes from the thin vein area (Fig. 12b) and the skin (Fig. 12c) was 0.875. That between the codes from the thick (Fig. 12a) and the thin vein areas (Fig. 12b) was 0.375. All of these HDs are greater than 0.138. In our system, if the HD of the input image is greater than 0.138, the input finger vein image is rejected as an un-enrolled one. The threshold was empirically determined and from this the minimum EER of recognition was obtained. From that, we can discern that the codes extracted from the thick vein, thin vein, and skin areas were different from each other and the vein information was actually being encoded by the proposed method.

Fig. 13 shows that the database was collected by the proposed acquisition process including the intra-class variations such as translation, rotation, and

rolling of the finger. The intra-variations by translation and rolling were reduced by using the image stretching and the bit shifting matching in the horizontal and vertical directions. Those by rotation were reduced using the LBP method (Jang YK *et al.*, 2008).

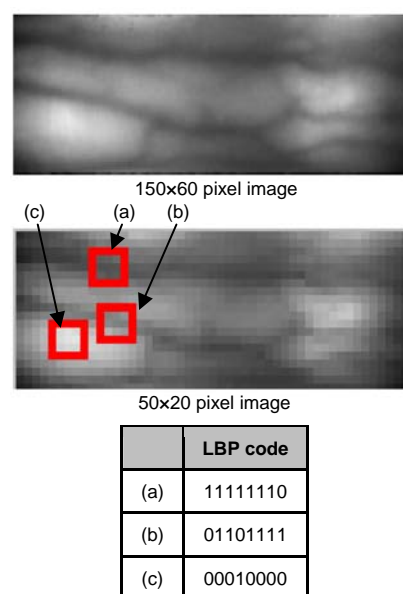


Fig. 12 Examples of the local binary pattern (LBP) codes from thick vein, thin vein, and skin areas

(a) Thick vein area; (b) Thin vein area; (c) Skin area

However, in the case of severe rotation (greater than 17°), rolling (greater than 15°), or translation (greater than +60 pixels) (which seldom occurs although allowing for natural movement of the finger when acquiring the image), false rejection can occur.

Fig. 13 shows some false rejection cases. In our system, if the HD of the input image is greater than 0.138, the input finger vein image is rejected as an un-enrolled one. This threshold was empirically determined by which the minimum EER of recognition was obtained. The receiver operational characteristic (ROC) curves are depicted in Fig. 14. It describes the genuine acceptance rate (GAR) (100%–false rejection rate) of all the finger vein methods at various false acceptance rate (FAR) levels. Here, FRR is the error rate of the non-acceptance of the genuine user as an un-enrolled one. The FAR is that of falsely regarding an imposter user as a correct user. Our recognition error is lower than those of the previous methods at all FAR levels, as shown in Fig. 14.

Fig. 15 and Tables 1 and 2 show that the proposed method outperforms the previous ones (Wang

et al., 2008; Jang YK et al., 2008; Lee et al., 2009). In the case presented in Table 1, we performed genuine tests which meant that Figs. 15a and 15b came from the same finger of a user. Table 1 indicates that both Jang YK et al. (2008)'s method and the proposed one showed 'correct, accept'. Since the vein patterns were

not distinctive in the input image, the other previous methods of Wang et al. (2008) and Lee et al. (2009) showed a false rejection due to the incorrect detection of the vein patterns and vein minutia. These false rejections mean that the image is an enrolled one, but is not recognized.

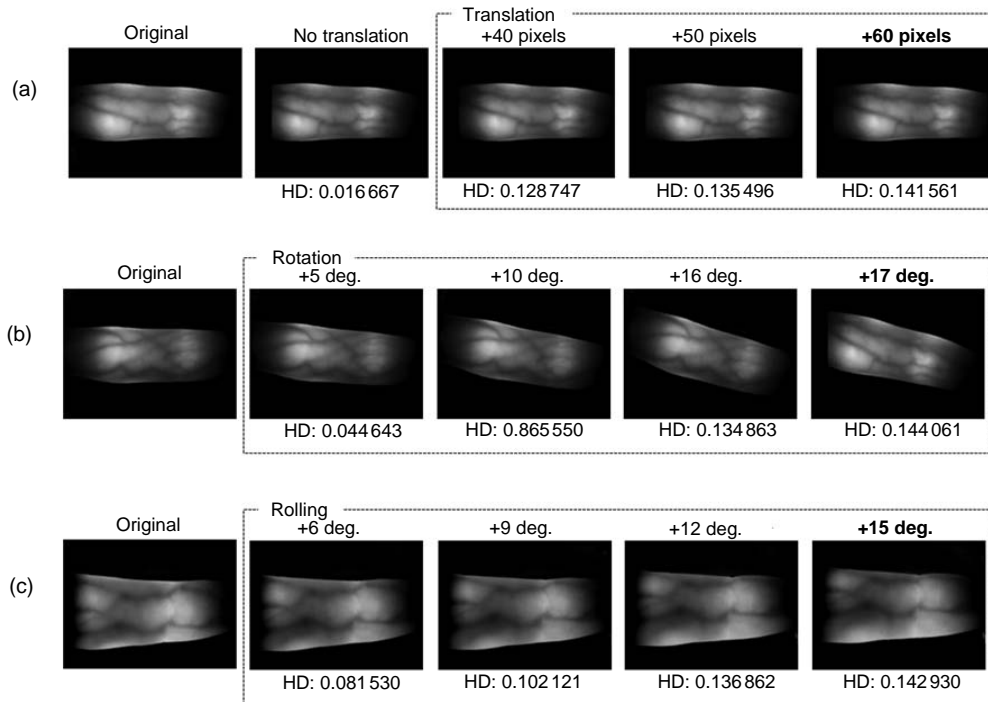


Fig. 13 The changes of the hamming distances of the same finger in case of (a) translation, (b) rotation, and (c) rolling

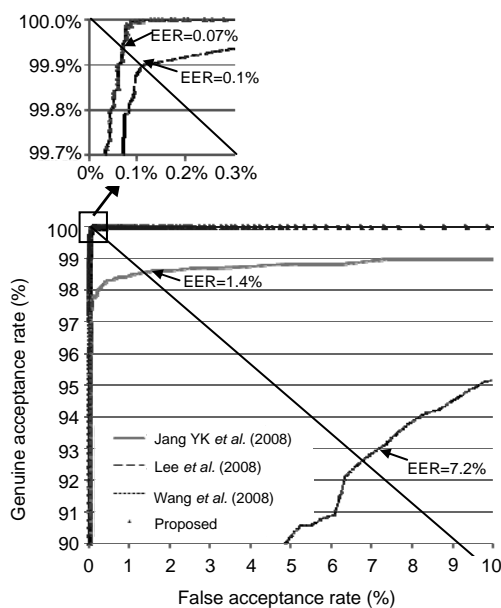


Fig. 14 Receiver operational characteristic (ROC) curves

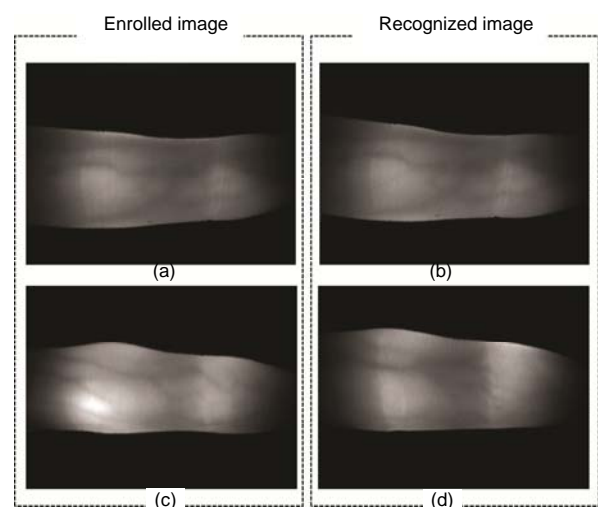


Fig. 15 Examples of genuine and imposter tests
 (a) Enrolled image 1; (b) Corresponding recognized image 1;
 (c) Enrolled image 2; (d) Corresponding recognized image 2

Table 1 Genuine test referring to Figs. 15a and 15b

Method	Result
Jang YK <i>et al.</i> (2008)	Correct, accept
Lee <i>et al.</i> (2009)	False, reject
Wang <i>et al.</i> (2008)	False, reject
Proposed	Correct, accept

Table 2 Imposter test referring to Figs. 15c and 15d

Method	Result
Jang YK <i>et al.</i> (2008)	False, accept
Lee <i>et al.</i> (2009)	False, accept
Wang <i>et al.</i> (2008)	False, accept
Proposed	Correct, reject

In the case presented in Table 2, we performed imposter tests which meant that Figs. 15c and 15d came from a different finger. As shown in Table 2, only the proposed one showed the results of a correct rejection. Since the vein patterns are not distinctive in the input image, the previous methods (Wang *et al.*, 2008; Lee *et al.*, 2009) revealed false acceptance due to the incorrect detection of vein patterns and vein minutia. False acceptance means that the image is not an enrolled one, but is falsely recognized as an enrolled one. Since the proposed method uses the weighted LBP method based on SVM, its capability to discriminate imposter images was better than that of the previous method which used the simple LBP method (Jang YK *et al.*, 2008).

The proposed method uses weighted LBP codes. The weights were determined in Fig. 10 based on the vein patterns included in local area in which the LBP codes were extracted. On the contrary, the previous methods (Wang *et al.*, 2008; Jang YK *et al.*, 2008; Lee *et al.*, 2009) did not use the weights for the LBP codes or the MHD distance. Since, in general, the LA area in which a large amount of vein is included has a greater effect on the recognition performance than the area in which a smaller amount of vein is included such as in the SA or MA, the degree of effect is represented by the weights on the LBP codes in our study. The experimental results (Fig. 14) showing that our recognition error was lower than those of the previous methods (Wang *et al.*, 2008; Jang YK *et al.*, 2008; Lee *et al.*, 2009) confirm our analyses.

The processing time was compared on a desktop computer with a Pentium IV 3 GHz main processor. The size of main memory was 1 GB (Table 3). The processing time of the proposed method was 72.5 ms

and was similar to that of the previous method based on the simple LBP codes of Jang YK *et al.* (2008).

The previous methods using bifurcation and ending points took much longer time for extracting and aligning vein patterns (Lee *et al.*, 2009). The proposed method had a longer processing time than Wang *et al.* (2008)'s method but its processing speed was faster than those of Jang YK *et al.* (2008) and Lee *et al.* (2009).

Table 3 Comparison of processing time

Method	Processing time (ms)
Jang YK <i>et al.</i> (2008)	91.4
Lee <i>et al.</i> (2009)	118.6
Wang <i>et al.</i> (2008)	56.4
Proposed	72.5

4 Conclusions

We have proposed a new vein identification method with weighted LBP codes. Using an SVM, a local area of 3×3 pixels of a finger region were classified into large amounts (LA), medium amounts (MA), and small amounts (SA) of vein patterns. In our experiments, we obtained an equal error rate of 0.049%. The processing time was 72.5 ms.

The thickness of vein can be changed according to blood flow, which varies by weather or the health of the user. The recognition accuracy of the proposed method can be reduced by these variations because only the texture information of the vein is used. Thus, we plan to develop a method which is not affected by vein thickness.

References

- Ahonen, T., Hadid, A., Pietikäinen, M., 2006. Face description with local binary patterns: application to face recognition. *IEEE Trans. Pattern Anal. Mach. Intell.*, **28**(12):2037-2041. [doi:10.1109/TPAMI.2006.244]
- Choi, J.H., Song, W.S., Kim, T.J., Lee, S.R., Kim, H.C., 2009. Finger vein extraction using gradient normalization and principal curvature. *SPIE*, **7251**:1-9. [doi:10.1117/12.810458]
- Ding, Y., Zhuang, D., Wang, K., 2005. A Study of Hand Vein Recognition Method. Proc. IEEE Int. Conf. on Mechatronics and Automation, p.2106-2110. [doi:10.1109/ICMA.2005.1626888]
- Dubuisson, M.P., Jain, A.K., 1994. A Modified Hausdorff Distance for Object Matching. Proc. 12th Int. Conf. on Pattern Recognition, p.566-568. [doi:10.1109/ICPR.1994.

- 576361]
- Ferrer, M.A., Morales, A., Ortega, L., 2009. Infrared hand dorsum images for identification. *Electron. Lett.*, **45**(6): 306-308. [doi:10.1049/el.2009.0136]
- Guo, G., Jones, M.J., 2008. Iris Extraction Based on Intensity Gradient and Texture Difference. Proc. IEEE Workshop on Applications of Computer Vision, p.1-6. [doi:10.1109/WACV.2008.4544018]
- Huttenlocher, D.P., Klanderman, G.A., Rucklidge, W.A., 1993. Comparing images using the Hausdorff distance. *IEEE Trans. Pattern Anal. Mach. Intell.*, **15**(9):850-863. [doi:10.1109/34.232073]
- Jain, A.K., Ross, A., Prabhakar, S., 2004. An introduction to biometric recognition. *IEEE Trans. Circ. Syst. Video Technol.*, **14**(1):4-19. [doi:10.1109/TCSVT.2003.818349]
- Jang, J., Park, K.R., Kim, J., Lee, Y., 2008. New focus assessment method for iris recognition systems. *Pattern Recogn. Lett.*, **29**(13):1759-1767. [doi:10.1016/j.patrec.2008.05.005]
- Jang, Y.K., Kang, B.J., Park, K.R., 2008. A study on touchless finger vein recognition robust to the alignment and rotation of finger. *KIPS Trans. Part B*, **15-B**(4):275-284.
- Kang, B.J., Park, K.R., 2009. Multimodal biometric authentication based on the fusion of finger vein and finger geometry. *Opt. Eng.*, **48**(9):090501. [doi:10.1117/1.3212651]
- Lee, E.C., Park, K.R., 2009. Restoration method of skin scattering blurred vein image for finger vein recognition. *Electron. Lett.*, **45**(21):1074-1076. [doi:10.1049/el.2009.1231]
- Lee, E.C., Lee, H.C., Park, K.R., 2009. Finger vein recognition by using minutia based alignment and local binary pattern-based feature extraction. *Int. J. Imag. Syst. Technol.*, **19**(3):179-186. [doi:10.1002/ima.20193]
- Lin, C., Fan, K., 2004. Biometric verification using thermal images of palm-dorsa vein patterns. *IEEE Trans. Circ. Syst. Video Technol.*, **14**(2):199-213. [doi:10.1109/TCSVT.2003.821975]
- Miura, N., Nagasaka, A., Miyatake, T., 2004. Feature extraction of finger-vein patterns based on repeated line tracking and its application to personal identification. *Mach. Vis. Appl.*, **15**(4):194-203. [doi:10.1007/s00138-004-0149-2]
- Miura, N., Nagasaka, A., Miyatake, T., 2007. Extraction of finger-vein patterns using maximum curvature points in image profiles. *IEICE Trans. Inform. Syst.*, **E90-D**(8): 1185-1194. [doi:10.1093/ietisy/e90-d.8.1185]
- Ojala, T., Pietikäinen, M., Harwood, D., 1996. A comparative study of texture measures with classification based on featured distributions. *Pattern Recog.*, **29**(1):51-59. [doi:10.1016/0031-3203(95)00067-4]
- Ojala, T., Pietikäinen, M., Maenpaa, T., 2002. Multiresolution gray-scale and rotation invariant texture classification with local binary patterns. *IEEE Trans. Pattern Anal. Mach. Intell.*, **24**(7):971-987. [doi:10.1109/TPAMI.2002.1017623]
- Solla, S.A., Leen, T.K., Müller, K., 2000. Advances in Neural Information Processing Systems 12. MIT Press, Cambridge, p.834-840.
- Sukumaran, S., Punithavalli, M., 2009. Retina recognition based on fractal dimension. *Int. J. Comput. Sci. Network Secur.*, **9**(10):66-70.
- Usher, D., Tosa, Y., Friedman, M., 2008. Ocular Biometrics: Simultaneous Capture and Analysis of the Retina and Iris. Advances in Biometrics. Springer, London. [doi:10.1007/978-1-84628-921-7_8]
- Vapnik, V., 1998. Statistical Learning Theory. John Wiley & Sons, New York.
- Wang, L., Leedham, G., 2006. Near- and Far-Infrared Imaging for Vein Pattern Biometrics. Proc. IEEE Int. Conf. on Video and Signal Based Surveillance, p.52. [doi:10.1109/AVSS.2006.80]
- Wang, L., Leedham, G., Cho, D.S.Y., 2008. Minutiae feature analysis for infrared hand vein pattern biometrics. *Pattern. Recog.*, **41**(3):920-929. [doi:10.1016/j.patcog.2007.07.012]
- Watanabe, M., 2008. Palm Vein Authentication. Advances in Biometrics. Springer, London. [doi:10.1007/978-1-84628-921-7_5]
- Yanagawa, T., Aoki, S., Ohyama, T., 2007. Human Finger Vein Images Are Diverse and Its Patterns Are Useful for Personal Identification. MHF Preprint Series, MHF 2007-12, 21st Century COE Program, Development of Dynamic Mathematics with High Functionality, Kyushu University, Korea.
- Yang, H., Wang, Y., 2007. A LBP-Based Face Recognition Method with Hamming Distance Constraint. Proc. 4th Int. Conf. on Image and Graphics, p.645-649. [doi:10.1109/ICIG.2007.144]
- Zhang, Z., Ma, S., Han, X., 2006. Multiscale Feature Extraction of Finger-Vein Patterns Based on Curvelets and Local Interconnection Structure Neural Network. Proc. 18th Int. Conf. on Pattern Recognition, p.145-148. [doi:10.1109/ICPR.2006.848]